Dynamics of ESCRT protein recruitment during retroviral assembly

Nolwenn Jouvenet[1,2], Maria Zhadina[1], Paul D. Bieniasz[1,3,5] and Sanford M. Simon[4,5]

The ESCRT (endosomal sorting complex required for transport) complexes and associated proteins mediate membrane scission reactions, such as multivesicular body formation, the terminal stages of cytokinesis and retroviral particle release. These proteins are believed to be sequentially recruited to the site of membrane scission, and then complexes are disassembled by the ATPase Vps4A. However, these events have never been observed in living cells, and their dynamics are unknown. By quantifying the recruitment of several ESCRT and associated proteins during the assembly of two retroviruses, we show that Alix progressively accumulated at viral assembly sites, coincident with the accumulation of the main viral structural protein, Gag, and was not recycled after assembly. In contrast, ESCRT-III and Vps4A were transiently recruited only when the accumulation of Gag was complete. These data indicate that the rapid and transient recruitment of proteins that act late in the ESCRT pathway and carry out membrane fission is triggered by prior and progressive accumulation of proteins that bridge viral proteins and the late-acting ESCRT proteins.

The ESCRT (endosomal sorting complex required for transport) complexes and associated proteins function in membrane fission events, such as multivesicular body (MVB) formation and the terminal stages of cytokinesis[1,2]. The ESCRT machinery is also required for the budding of numerous enveloped viruses, to cut the membranous neck that connects the virion to the plasma membrane[3,4]. There are more than 20 ESCRT members in mammalian cells and they are all connected into a coherent network by protein–protein interactions[5]. The network consists of three complexes, ESCRT-I, ESCRT-II and ESCRT-III, and other associated proteins such as the ATPase vacuolar protein sorting 4 (Vps4). ESCRT proteins are soluble and are thought to be recruited at the site of membrane fission in an ordered manner[6–8], with ESCRT-I proteins (such as tumour susceptibility gene 101, Tsg101) and associated proteins (Alix) acting early in the pathway, and ESCRT-III proteins (charged MVB proteins, Chmp) acting late, and then disassembled by the ATPase Vps4A (ref. 9). Indeed, recent *in vitro* data indicate that ESCRT-III proteins are responsible for the scission of the membrane neck and that Vps4 acts after the scission step to recycle the complex[10,11]. However, the *in vivo* kinetics of assembly and disassembly of ESCRT proteins at site of membrane fission is unknown. There are no direct observations available to support the idea that there is a sequential recruitment of the ESCRT machinery to viral assembly sites, or during MVB formation or cytokinesis. The recycling of ESCRT proteins by Vps4 has not been directly observed in live cells either.

Numerous enveloped viruses, including all retroviruses[3,4], hijack the ESCRT machinery for budding. Retroviruses recruit the machinery through specific sequences, called late domains, that are contained within their main structural protein, Gag[3,4]. There are three known types of late domain that all recruit different ESCRT proteins through direct interactions: Pro–Thr–Ala–Pro (PTAP) sequences recruit Tsg101 (refs 12,13), Tyr–Pro–Asn–Leu or Leu–X–X–Leu–Phe (LXXLF) sequences recruit Alix[14,15] and Pro–Pro–X–Tyr interacts with ubiquitin ligases, such as Trp–Trp-domain-containing protein-1 (WWP1; ref. 16). Human immunodeficiency virus 1 (HIV-1) Gag contains two late domains, PTAP and LXXLF, with PTAP being the functionally more important motif[3,4] and recruiting the ESCRT complex through a direct interaction with Tsg101 (refs 12, 13). The second late domain, LXXLF, interacts with Alix[14,15]. The retrovirus equine infectious anaemia virus (EIAV) Gag possesses a unique Tyr–Pro–X–Leu (YPXL) late domain, which recruits the ESCRT complexes through a direct interaction with Alix[14,15,17,18]. In mammalian cells, Alix in turn recruits ESCRT-III proteins[14,17,18].

The assembly of HIV-1 and EIAV virions or virus-like-particles (VLPs) is driven by Gag proteins and takes place at the plasma membrane[19–21]. Using total-internal-reflection fluorescence microscopy (TIR-FM), which selectively excites fluorophores near the coverslip (within ~ < 70 nm; ref. 22) and carboxy-terminally tagged fluorescent versions of Gag in transfected HeLa cells[23], there is sufficient
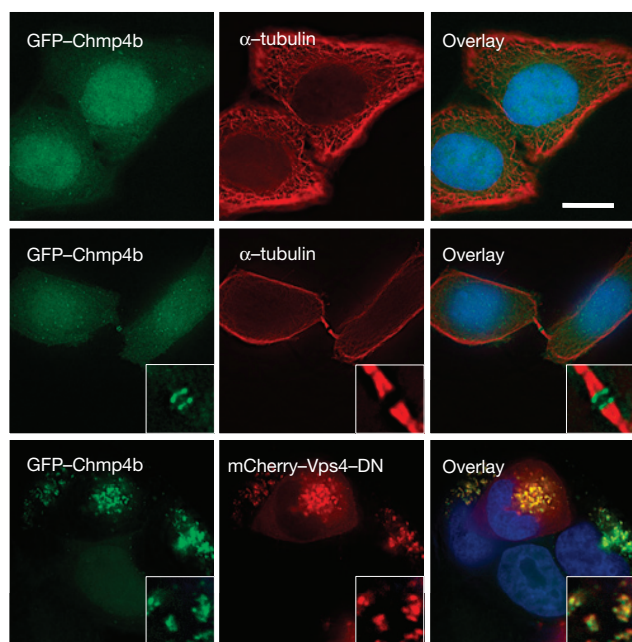
Figure 1 Characterization of the GFP–Chmp4b-expressing cell clone. HeLa cells stably expressing GFP–Chmp4b (green) were fixed and stained with anti-α-tubulin antibodies (red) and with DAPI (blue). Images show the distribution of GFP–Chmp4b in interphase cells (top panels) and in telophase cells (middle panels). Alternatively, cells were transfected with mCherry–Vps4-DN (bottom panels), fixed 18 h post-transfection and stained with DAPI (blue). Samples were observed with an epifluorescence microscope. Deconvolved optical sections acquired at the centre of the vertical dimension of the cell are shown. Expanded views are shown in insets. Scale bar, 10 μm.

signal-to-noise ratio to allow dynamic quantification of the assembly of individual VLPs, from initiation of assembly to budding and release[23–25]. We have previously determined, using fluorescence recovery after photobleaching analysis, that completion of particle assembly occurs when the recruitment of Gag molecules stops, which corresponds to the point when the intensity of the Gag signal reaches a plateau[23]. The time to complete assembly is the elapsed time from the first image at which a fluorescent puncta is first detectable to the point when its intensity reaches a plateau.

Here, we quantified the recruitment of ESCRT and associated proteins during the assembly of mCherry-tagged HIV-1 and EIAV VLPs using cell lines stably expressing green fluorescent protein (GFP)-fused ESCRT proteins. These studies reveal that there are two clearly distinct behaviours among members of the ESCRT pathway and that the Vps4 removes some, but not all, ESCRT pathway components from sites of viral budding.

RESULTS

Characterization of cell lines stably expressing GFP-tagged ESCRT proteins

Our goal was to use fluorescence microscopy to determine the dynamics of ESCRT protein recruitment during assembly of HIV-1 and EIAV VLPs. However, overexpression of ESCRT proteins fused to bulky tags such as fluorescent proteins can be deleterious to cell physiology and virion release[14,17,26–28]. Thus, we established criteria for selecting fusion proteins and stable cell lines for our analyses. First, the GFP-tagged

ESCRT proteins had to interact with the endogenous components of the ESCRT pathway, as assessed by localization of the GFP–ESCRT fusion protein to the midbody during cytokinesis (Fig. 1 and Supplementary Figs S1–S4) and recruitment to class E compartments, induced by expression of a catalytically inactive dominant-negative Vps4A[E228Q] mutant (Vps4A-DN). Second, there had to be no gross effects on cell physiology or division (Fig. 2a,b) or on the kinetics of HIV-1 VLP assembly or release (Fig. 2c,d) that sometimes accompany ESCRT protein overexpression[29,30]. Third, the GFP fusion proteins had to remain intact, as assayed by western blot assays (Supplementary Fig. S5a). Fourth, all of the cells of a clone had to express relatively homogeneous level of the fluorescent proteins (Supplementary Fig. S5b). Finally, in situations where antibodies to the ESCRT protein were available, the level of expression of the GFP-tagged ESCRT protein had to be close to the level of the native protein, as assayed by western blot analysis (Supplementary Fig. S5c).

On the basis of these criteria, clonal cell lines were developed that stably expressed Alix, Chmp1b, Chmp4b, Chmp4c, Chmp6, Tsg101 and Vps4A, each fused to GFP. Each cell clone exhibited either a diffuse cytoplasmic fluorescence (Tsg101, Alix, Chmp4c and Chmp6) or diffuse cytoplasmic and nuclear fluorescence (Chmp1b, Chmp4b and Vps4A; Fig. 1 and Supplementary Figs S1–S4) when imaged by epi-illumination. Some bright cytoplasmic GFP puncta were also detected in each cell line, possibly representing endosomes or centrosomes[31] (Fig. 1 and Supplementary Figs S1–S4). Using TIR-FM, these GFP puncta occasionally appeared transiently in the vicinity of the plasma membrane. As expected[27], when co-expressed with mCherry–Vps4A-DN, each of these GFP-fused ESCRT fusion proteins accumulated on a characteristic class E compartment (Fig. 1 and Supplementary Figs S1–S4). Moreover, as previously reported[32,33], these GFP-tagged proteins localized to the midbody at late stages of cell division (Fig. 1 and Supplementary Figs S1–S4).

Association of some ESCRT proteins with HIV-1 and EIAV Gag is transient owing to the action of Vps4

When cells stably expressing GFP-tagged ESCRT proteins were transiently transfected with a mixture of plasmids expressing HIV-1 Gag and Gag–mCherry and imaged at a single time point, fluorescent puncta of some of the GFP–ESCRT proteins (specifically GFP–Chmp4b, GFP–Chmp4c and Chmp1b–GFP) were observed at the plasma membrane, as visualized by TIR-FM. Most of the fluorescent puncta of GFP–ESCRT co-localized with puncta of Gag–mCherry (Fig. 3a top row, Fig. 3b). However, the converse was not the case. At many puncta of Gag–mCherry, the GFP–ESCRT fusion proteins were not detectable (Fig. 3a top row, Fig. 3b). In contrast, when a catalytically inactive Vps4A-DN was also expressed, GFP–Chmp4b puncta were detected at most Gag–mCherry puncta (Fig. 3a bottom row, Fig. 3b). Similarly, Chmp1b–GFP and GFP–Chmp4c puncta co-localized with HIV-1 Gag–mCherry puncta, but most of the Gag–mCherry puncta co-localized with the Chmp1b–GFP and GFP–Chmp4c puncta, only when Vps4A-DN was also expressed (Fig. 3b). There was no detectable GFP signal co-localized with HIV-1 Gag–mCherry puncta in the cell lines expressing GFP–Tsg101, GFP–Alix or Chmp6–GFP.

When EIAV Gag/Gag–mCherry were used in place of HIV-1 Gag, a similar pattern of co-localization was observed with GFP-tagged
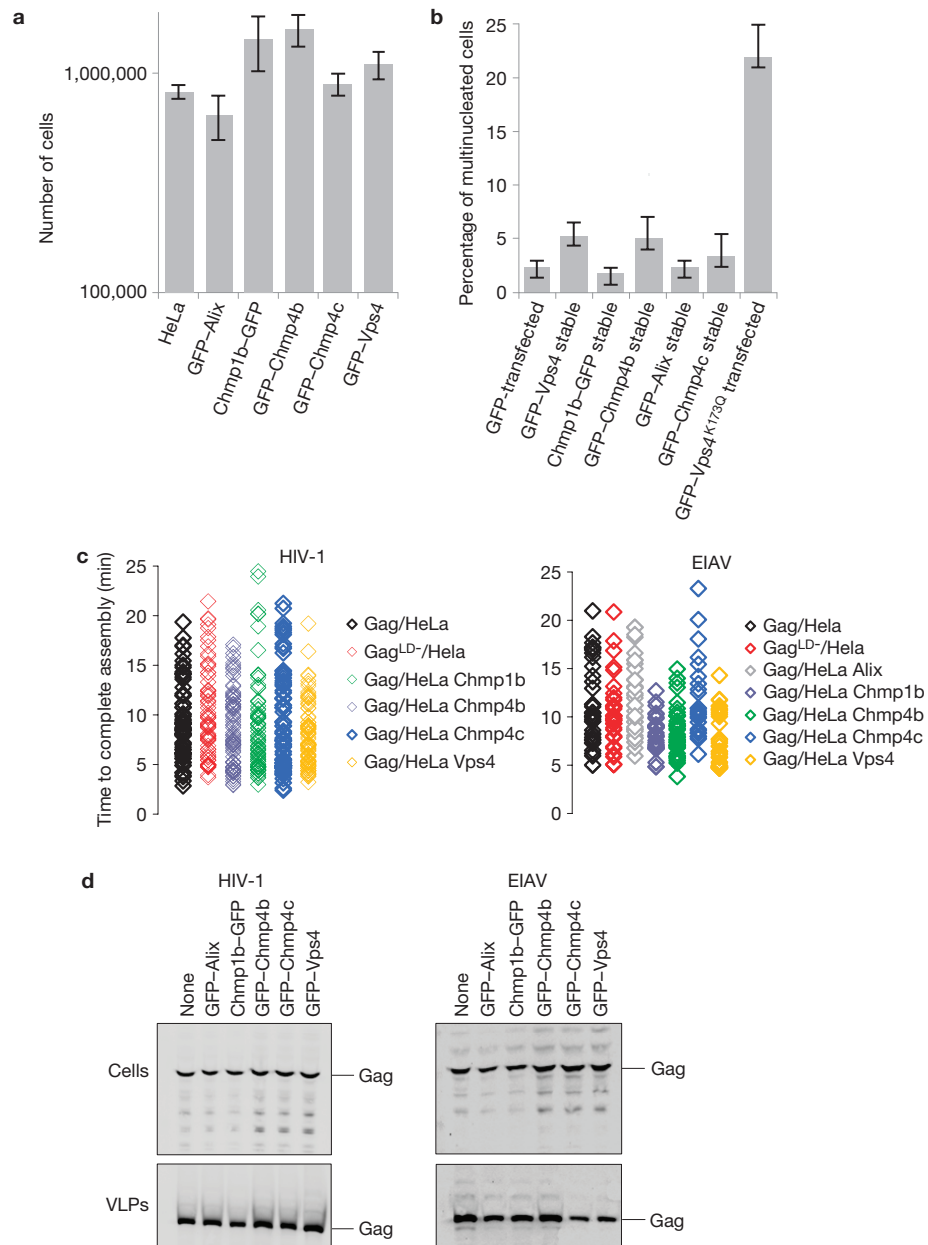
Figure 2 Effect of stably expressed GFP-fused ESCRT proteins on cell proliferation, cytokinesis and virion assembly and release. (**a**) The stable expression of GFP-tagged ESCRT proteins does not affect cell proliferation. Cells (10^5) were plated into each well of a 24-well plate, collected and counted 48 h later. Error bars indicate s.d. from three independent experiments. (**b**) Stable expression of GFP-tagged ESCRT proteins does not disrupt cytokinesis. HeLa cells stably expressing GFP-tagged ESCRT proteins or transfected with GFP or GFP–Vps4^{K173Q} were fixed, stained with both anti-α-tubulin antibodies and DAPI, and scored for multinucleated cells. Three-hundred cells from three independent experiments were analysed for the presence of more than one nucleus per cell for each factor. Error bars indicate s.d. (**c**) Kinetics of HIV-1 and EIAV assembly were not affected in the cell lines stably expressing GFP-tagged ESCRT proteins. The plots show the time to complete assembly for individual HIV-1 and EIAV VLPs, including wild-type and late-domain mutant (LD-) Gag proteins, in unmodified HeLa cells, or cell lines expressing the indicated GFP–ESCRT protein lines. Each symbol represents an individual VLP. The time to complete assembly was defined for each VLP as the interval between the points of inflection on plots of fluorescence intensity as a function of time. (**d**) The cell lines stably expressing GFP-tagged ESCRT proteins support the release of HIV-1 and EIAV Gag VLPs. Western blot analysis of HeLa cells and HeLa cells stably expressing GFP-tagged ESCRT transfected with HIV-1 (left panel) or EIAV (right panel) Gag. Samples were probed with an anti-p24 monoclonal antibody for HIV-1 or anti-EIAV horse serum. Supplementary Fig. S6 shows the corresponding unprocessed western blots.

Chmp1b, Chmp4b, Chmp4c and Vps4A. Namely, most GFP–Chmp protein puncta localized with Gag puncta, but only a subset of Gag puncta localized with Chmp protein puncta. In contrast, GFP–Alix puncta were observed coincident with nearly all EIAV Gag puncta, even in the absence of Vps4A-DN (Supplementary Fig. 4c).

These results indicated that the association of many of the ESCRT proteins, particularly the Chmp proteins, with Gag might be transient, but stabilized when Vps4A activity was inhibited. Thus, we examined the dynamics of the localization of the ESCRT proteins, during assembly of VLPs.
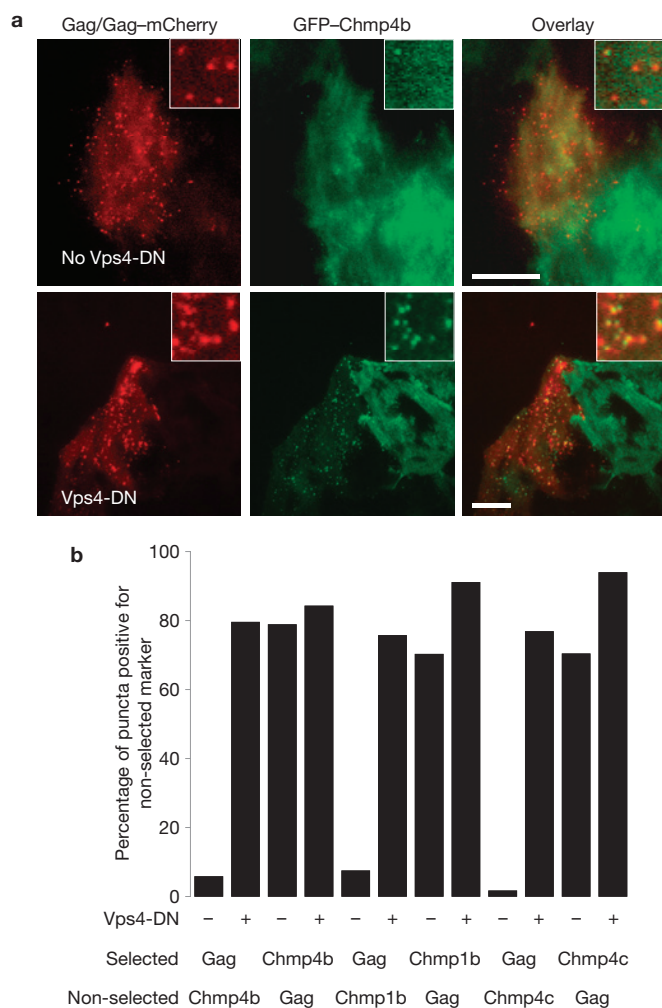
Figure 3 Catalytically inactive Vps4A increases localization of stably expressed GFP-tagged ESCRT-III proteins at sites of HIV-1 assembly. (**a**) HeLa cells stably expressing GFP-Chmp4b (green) were transfected with HIV-1 Gag/Gag-mCherry (red), in the absence (top panel) or presence (bottom panel) of Vps4A-DN. Cells were fixed 24 h later and observed with a TIR-FM microscope. Expanded views are shown in insets. Scale bars, 10 μm. (**b**) Quantification of the co-localization between VLPs and puncta of ESCRT proteins. HeLa cells stably expressing GFP-fused ESCRT-III proteins were transfected with Gag/Gag-mCherry, in the absence (−) or presence (+) of Vps4A-DN, as indicated. Cells were observed under TIR-FM at 18 h post-transfection and the co-localization between puncta of Gag-mCherry and puncta of GFP was quantified by randomly selecting puncta of one marker (selected) and then enumerating the percentage of these puncta that were coincident with puncta of the other, non-selected marker.

Dynamics of HIV-1 and EIAV assembly

We have previously published criteria for assaying HIV-1 particle assembly by following the quantitative recruitment of Gag, and demonstrated that Gag recruitment into nascent VLPs becomes irreversible once it reaches a plateau (by fluorescence recovery after photobleaching) and that Gag is closely packed in VLPs (by FRET; ref. 23).

Similarly to our previous findings[23,24], recruitment of HIV-1 Gag/Gag-mCherry into individual VLPs was completed in a mean of 9.6 min after the initial detection of a punctum ($n = 65$, range 4–19.4 min, Fig. 2c). EIAV Gag assembly was similarly completed in a

mean of 11.5 min ($n = 36$, range 5–21.4 min; Fig. 2c). In both cases, the rate of VLP assembly was indistinguishable in unmodified cells when compared to those expressing the GFP-ESCRT proteins (Fig. 2c).

Interestingly, the assembly kinetics of VLPs composed of late-domain-deficient HIV-1 Gag (10.6 min, range 4.2–21.5 min, $n = 63$) and EIAV Gag (10.4 min, range 5–21.2 min, $n = 34$; Fig. 2c), was indistinguishable from the 9.6 min and 11.5 min assembly kinetics of the corresponding wild-type HIV-1 and EIAV VLPs. This finding is similar to a previous report[25] and indicates that the ESCRT proteins do not affect the rate of assembly.

Dynamics of ESCRT protein recruitment during retroviral assembly

When HIV-1 VLP assembly was imaged in cells stably expressing Chmp1b-GFP, GFP-Chmp4b, GFP-Chmp4c or GFP-Vps4A, there was a transient increase of GFP fluorescence at nascent HIV-1 VLPs. This transient appearance of GFP-tagged ESCRT proteins was, typically, coincident with the termination of the recruitment of Gag to the corresponding VLP (Fig. 4). The dynamics of the recruitment of Chmp1b-GFP, GFP-Chmp4b, GFP-Chmp4c or GFP-Vps4A to nascent EIAV VLPs was strikingly similar to that observed with HIV-1 (Fig. 5). At each VLP there was transient recruitment of each GFP-ESCRT fusion protein at the site of VLP assembly, close to the termination of EIAV Gag recruitment.

The aforementioned Chmp and Vps4A proteins are not thought to bind directly to Gag. Rather, HIV-1 and EIAV Gag proteins engage the ESCRT machinery through late domains that directly bind Tsg101 (PTAP in HIV-1; refs 12,13,34) or Alix (LXXLF in HIV-1, YPXL in EIAV; refs 14,15,17,18). These late-domain-binding proteins are presumed to act as bridging factors to the ESCRT-III proteins that are responsible for membrane scission. Indeed, interactions between Alix and Chmp4 proteins are well described[14,17,18] and are essential for the ability of Alix to promote HIV-1 release and cytokinesis[15,35,36].

On expression of HIV-1 Gag-mCherry in cell lines expressing GFP-Tsg101 or GFP-Alix, we were not able to detect either GFP fusion protein at sites of HIV-1 Gag-mCherry VLP assembly. Presumably, the numbers of molecules of GFP-Tsg101 or GFP-Alix that were recruited fell below the detection threshold. The EIAV late domain (YPXL) has a higher affinity for Alix than does the HIV-1 LXXLF motif[17,37] and we were readily able to detect GFP-Alix recruitment to EIAV VLPs. The dynamics of Alix recruitment was completely different from those of Chmp and Vps4A protein recruitment. Specifically, Alix progressively accumulated at the sites of VLP assembly with the same dynamics as Gag, and remained there throughout the period of observation (Fig. 6).

We next quantified the time at which each ESCRT protein appeared and disappeared relative to the termination of HIV-1 and EIAV Gag recruitment (Fig. 7a, $n = 477$). All of the ESCRT-III proteins (Chmp1b, Chmp4b, Chmp4c), as well as Vps4A, were recruited transiently at approximately the same time as recruitment of HIV-1 or EIAV Gag ended, whereas Alix was recruited at the same time as Gag and remained detectable at all VLPs thereafter (Fig. 7a).

Notably, ESCRT protein recruitment was observed at most assembling VLPs. Specifically, Alix recruitment was detectable in 100% of EIAV assembly events ($n = 36$) and recruitment of ESCRT-III/Vps4A was detectable in 84% ($n = 441$) of HIV-1 and EIAV assembly events (Fig. 7b). In contrast, the recruitment of each of these ESCRT

397
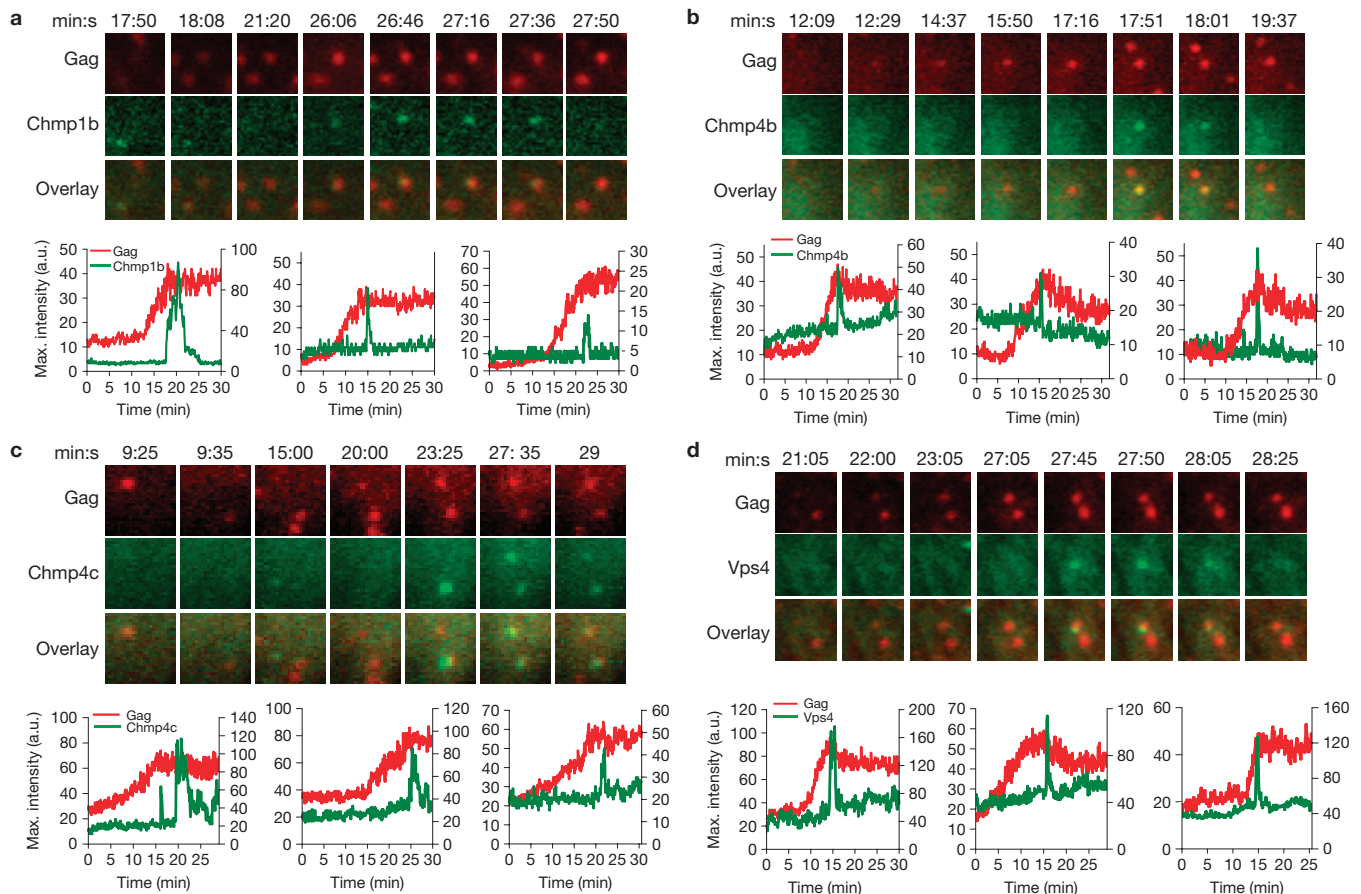
Figure 4 Imaging Chmp1b, Chmp4b, Chmp4c and Vps4A recruitment during HIV-1 Gag assembly. (**a–d**) HeLa cells stably expressing Chmp1b–GFP (**a**), GFP–Chmp4b (**b**), GFP–Chmp4c (**c**) or GFP–Vps4A (**d**) were transfected with HIV-1 Gag/Gag–mCherry and observed under TIR-FM beginning at 6 h post-transfection. Each set of images illustrates the recruitment of GFP-labelled ESCRT proteins (green) during the genesis of an individual VLP (red). The time after the commencement of observation is given in minutes:seconds. Fields are $2.5 \times 2.5\,\mu$m. Plots of fluorescence intensity in arbitrary units (a.u.) as a function of time for the GFP–ESCRT protein (green, right axis) and Gag–mCherry signals (red, left axis) associated with the assembly of three individual VLPs are shown.

and associated proteins was greatly reduced (to between 3–10% of assembly events, $n = 323$) when Gag mutants that lacked late domains (Fig. 7b) were used.

Quantification of the time course of residency at the membrane for each of the ESCRT III proteins, and Vps4A, showed that they are recruited for only ∼1–3 min, although Chmp4c seemed to persist for 1–2 min longer (Fig. 7a). The different dynamics of Alix recruitment during EIAV Gag assembly is consistent with its role as a bridge between Gag and Chmp4, and its apparent failure to dissociate from VLP assembly sites (Fig. 7c) is consistent with biochemical data[14,18], showing that it is incorporated into viral particles.

At most VLPs, a single pulse of GFP–ESCRT-III/Vps4 protein recruitment was observed, but occasionally a second, or even a third, pulse was detected (Fig. 7d, examples in Figs 4c and 5a, left panels).

DISCUSSION

The curvature of cellular membranes is away from the cytosol during formation of MVBs, formation of the cleavage furrow during cell division and during the budding of viruses off the plasma membrane. Common to each of these events is the recruitment of the ESCRT complexes and associated proteins[1,2]. There is considerable biochemical and genetic evidence for the involvement of these proteins in these

processes. However, studying the dynamics of the ESCRT molecules has been limited by the adverse effects of expression of fluorescently tagged forms of these proteins. Here, we demonstrate that cell lines stably expressing low levels of these proteins fused to fluorescent proteins show none of the potential adverse effects, thereby allowing the study of these molecules with live-cell microscopy.

At individual assembling retrovirus particles, the dynamics of recruitment of the ESCRT and associated proteins could be categorized into two groups. Alix, which acts early in the pathway and binds directly to Gag, was recruited along with the viral proteins and remained with the viral particles (Fig. 6). The recruitment of Vps4A and the ESCRT-III proteins (Chmps) showed a strikingly different dynamics. First, the Vps4A and ESCRT-III were recruited only concomitant with the termination of the recruitment of Gag (Fig. 7a). Second, the Vps4A and ESCRT-III were recruited transiently, with a typical residence time of a few minutes (Fig. 7a,c).

The ESCRT-III and Vps4 proteins were most often recruited in a single pulse. However, in rare cases, two or three pulses of recruitment were detected (Fig. 7d). The timings of the arrival and recycling of Vps4 and those of the Chmp proteins were not distinguishable under our conditions. Rather, they seemed to be tightly coupled temporally in their appearance at and disappearance from the membrane.
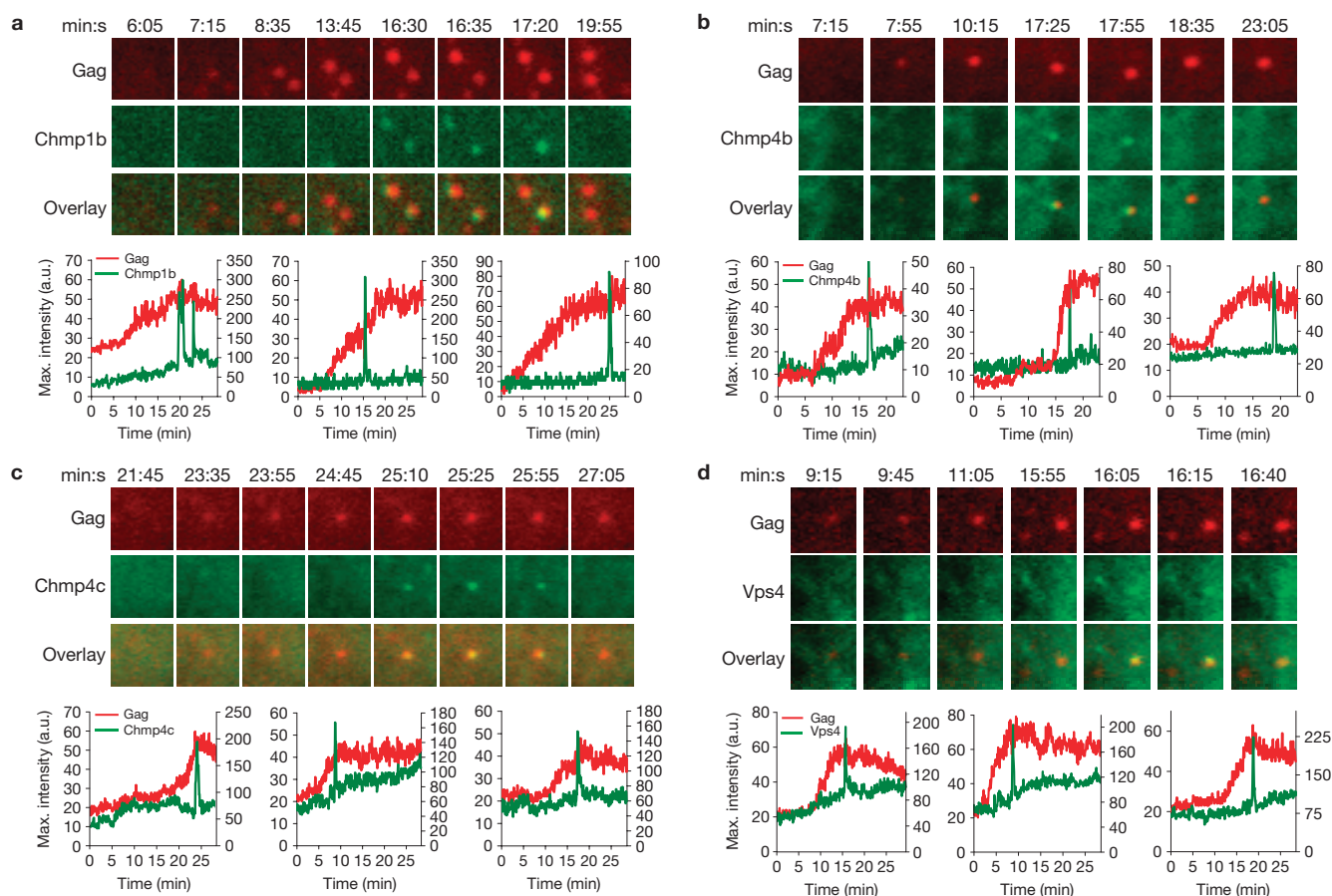
Figure 5 Imaging Chmp1b, Chmp4b, Chmp4c and Vps4A recruitment during EIAV Gag assembly. (**a–d**) HeLa cells stably expressing Chmp1b–GFP (**a**), GFP–Chmp4b (**b**), GFP–Chmp4c (**c**) or GFP–Vps4A (**d**) were transfected with EIAV Gag/Gag–mCherry and observed under TIR-FM beginning at 6 h post-transfection. Each set of images illustrates the recruitment of GFP-labelled ESCRT proteins during the genesis of an individual VLP. The time after the commencement of observation is given in minutes:seconds. Fields are $2.5 \times 2.5\,\mu m$. Plots of fluorescence intensity in arbitrary units (a.u.) as a function of time for the GFP–ESCRT protein (green, right axis) and Gag–mCherry signals (red, left axis) associated with the assembly of three individual VLPs are shown; the left graph in **a** and **d** corresponds to the microscopic images shown above.

Displacement of the ESCRT-III proteins is due to the ATPase activity of Vps4: in the presence of wild-type Vps4, the ESCRT-III proteins were observed only transiently at the membrane (Fig. 3). In contrast, in the presence of Vps4-DN, the ESCRT-III proteins were observed statically with many assembled Gag puncta (Fig. 3). Thus, it is possible that if the Vps4 is recruited or activated too quickly, the first pulse of recruitment of the ESCRT-III may be prematurely terminated, requiring another round of recruitment.

Interestingly, there was no diminution in the level of GFP–Alix associated with VLPs following the completion of assembly (Fig. 7a,c). This is consistent with previous findings that Alix is incorporated into HIV-1 particles with reasonable efficiency[14,18]. Conversely, the ESCRT-III and Vps4A proteins were most often completely removed from the site of assembly through the action of the ATPase (Fig. 7c). Thus, Vps4 seems to selectively remove ESCRT proteins, particularly those that are thought to mediate the membrane fission reaction, from the fission site. Occasionally, residual molecules of ESCRT-III and Vps4 were observed to remain co-localized with VLPs after assembly was apparently completed. However, this almost always constituted a small minority of the ESCRT-III and Vps4 molecules that were present at the peak of recruitment. From our results, it cannot be determined whether these molecules were left associated with the cytosolic membrane or within the nascent virion.

The ESCRT-III and Vps4A proteins were detectable at 84% of HIV-1 and EIAV assembly events (Fig. 7b). Moreover, the intensity of the signal emitted by each ESCRT proteins varied greatly from one assembly event to another, even within a single cell. Possibly, this could be explained by heterogeneity in the ratio of GFP-tagged proteins/endogenous proteins in individual budding events. Alternatively, there may be an overlap of function between the different ESCRT-III proteins and they may be recruited to varying degrees at different budding sites. Thus, in those assembly events where they were not detected, it may be that the fraction of the GFP-tagged ESCRT protein examined in that particular assembly event was below our detectable limit. A further source of heterogeneity may derive from variability in the number of ESCRT molecules recruited. Potentially the number recruited at assembly sites is determined by the number of Gag molecules per virion, which is known to vary considerably[38].

Importantly, when mutant Gag proteins that lacked late domains were used, the recruitment of each of these ESCRT and associated proteins was greatly reduced (Fig. 7b), but not completely abolished. The residual apparent recruitment of ESCRT proteins by Gag mutants could be explained by the presence of another, less efficient, late
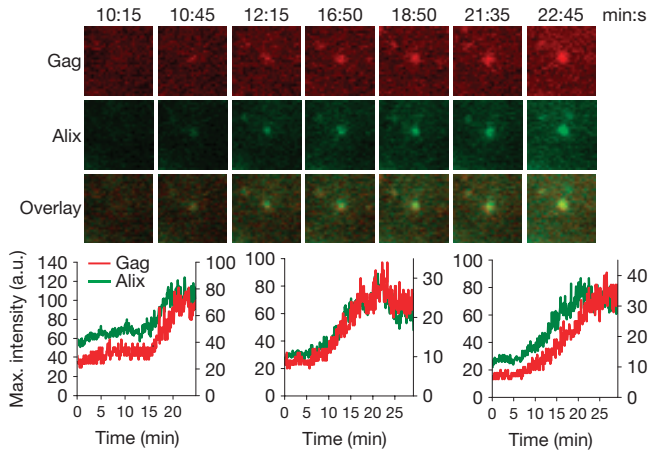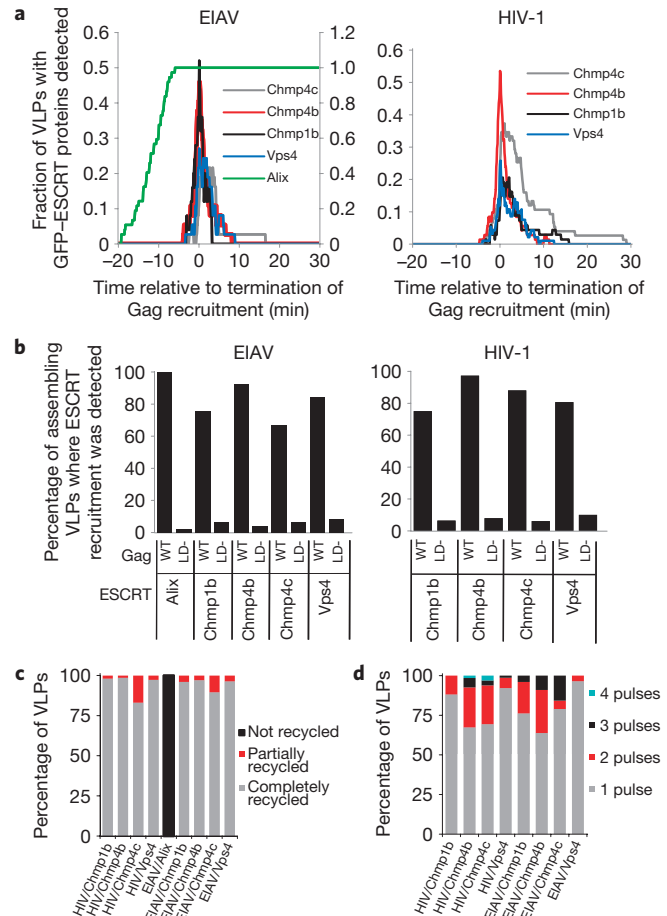
Figure 6 Imaging Alix recruitment during EIAV Gag assembly. HeLa cells stably expressing GFP–Alix were transfected with EIAV Gag/Gag–mCherry and observed under TIR-FM beginning at 6 h post-transfection. Each set of images illustrates the recruitment of GFP-labelled Alix proteins during the genesis of an individual VLP. The time after the commencement of observation is given in minutes:seconds. Fields are $2.5 \times 2.5\,\mu m$. Plots of fluorescence intensity in arbitrary units (a.u.) as a function of time for the GFP–Alix protein (green, right axis) and Gag–mCherry signals (red, left axis) associated with the assembly of three individual VLPs are shown; the left graph corresponds to the microscopic images shown above.

domain. Such a late domain, contained within the nucleocapsid domain of HIV-1 Gag and that can bind Alix, was recently described[39,40]. Another possibility is that some of these events might not represent proper recruitment, but rather the 'random' appearance of ESCRT puncta—which are observed in the absence of Gag at the plasma membrane—at the same location as assembling VLPs.

Two independent observations indicate that the ESCRT-III proteins do not play a role in initiation, execution or termination of recruitment of Gag. First, the ESCRT-III and Vps4A proteins were recruited only coincident with the completion of Gag accumulation (Fig. 7a). Thus, they are not likely to be involved in initiating or facilitating recruitment. If they were responsible for terminating Gag recruitment, the recruitment of Gag lacking a late domain should extend longer than the corresponding wild-type VLPs. However, the assembly kinetics of VLPs composed of mutant Gag (Fig. 2c) was indistinguishable from the assembly kinetics of wild-type VLPs. Similar findings were reported by others[25].

The expression of Vps4A-DN blocks release of virions from cells, indicating that Vps4 is required for particle release[13]. This could be explained by a requirement for Vps4 to remove ESCRT proteins, to enable the fission reaction, or recycle components of the ESCRT complexes from nascent virions for subsequent rounds of assembly. Alternatively, Vps4A-DN expression could result in the sequestration of ESCRT proteins on class E compartments. Thus, in the presence of Vps4A-DN, ESCRT proteins may simply not be available to mediate particle release. This hypothesis predicts that over time there should be an increase in VLPs that do not have ESCRT complexes associated with them. Our observations demonstrate that the presence of Vps4A-DN increases the number of ESCRT complexes that are observed to be associated with VLPs. This indicates that Vps4 plays a more active function in scission than simply recycling the ESCRT components.

Figure 7 Dynamics and pattern of ESCRT protein recruitment during retroviral assembly. (**a**) The fraction of EIAV (left panel) and HIV-1 (right panel) VLPs at which GFP–ESCRT protein was detectable, as a function of time. For this analysis, $T = 0$ was set as the point at which Gag recruitment to each VLP reached a plateau. (**b**) Percentage of VLP assembly events for which the recruitment of GFP-tagged ESCRT proteins was detected. HeLa cells stably expressing GFP-tagged ESCRT proteins were transfected with wild-type (WT) or late-domain mutant (LD−) HIV-1 (left panel) or EIAV (right panel) Gag/Gag–mCherry. Cells were observed live under TIR-FM beginning at 6 h post-transfection, for a period of 25–50 min. (**c**) Quantification of the number of pulses of ESCRT protein recruitment (percentage of VLPs for which each behaviour is observed) during HIV-1 and EIAV VLP assembly. (**d**) Removal of the GFP–ESCRT proteins from sites of HIV-1 and EIAV assembly. ESCRT-III and Vps4 proteins are generally completely recycled (as signified by the GFP signal at VLP assembly sites returning to baseline levels following the pulse), but in some cases, the proteins seem to be only partially recycled (for example Fig. 4c, images and left panel). Alix is not recycled (that is, the GFP signal remains at a plateau after reaching its maximum, see Fig. 6). The percentage of VLPs showing each behaviour is plotted.

Thus, our data support a model in which ESCRT-III functions may be limited to events after the recruitment of Gag. Our data are also consistent with a model in which the progressive accumulation of an 'early' ESCRT protein or complex (for example Alix or ESCRT-I) to a threshold level, potentially together with other factors (for example, curvature of the nascent virion or formation of a membranous neck), triggers the rapid deposition of ESCRT-III and Vps4A proteins that carry out membrane scission and ESCRT protein recycling. This model might be generalized to similar reactions at the MVB-limiting membrane and at the midbody and provides a simple

potential mechanism by which the fission machinery is temporally and spatially regulated. □

METHODS

Methods and any associated references are available in the online version of the paper at http://www.nature.com/naturecellbiology/

Note: Supplementary Information is available on the Nature Cell Biology website

1. McDonald, B. & Martin-Serrano, J. No strings attached: the ESCRT machinery in viral budding and cytokinesis. *J. Cell Sci.* **122,** 2167–2177 (2009).
2. Wollert, T. *et al*. The ESCRT machinery at a glance. *J. Cell Sci.* **122,** 2163–2166 (2009).
3. Bieniasz, P. D. Late budding domains and host proteins in enveloped virus release. *Virology* **344,** 55–63 (2006).
4. Morita, E. & Sundquist, W. I. Retrovirus budding. *Annu. Rev. Cell Dev. Biol.* **20,** 395–425 (2004).
5. Williams, R. L. & Urbe, S. The emerging shape of the ESCRT machinery. *Nat. Rev. Mol. Cell Biol.* **8,** 355–368 (2007).
6. Babst, M., Katzmann, D. J., Snyder, W. B., Wendland, B. & Emr, S. D. Endosome-associated complex, ESCRT-II, recruits transport machinery for protein sorting at the multivesicular body. *Dev. Cell* **3,** 283–289 (2002).
7. Babst, M., Katzmann, D. J., Estepa-Sabal, E. J., Meerloo, T. & Emr, S. D. Escrt-III: an endosome-associated heterooligomeric protein complex required for mvb sorting. *Dev. Cell* **3,** 271–282 (2002).
8. Katzmann, D. J., Babst, M. & Emr, S. D. Ubiquitin-dependent sorting into the multivesicular body pathway requires the function of a conserved endosomal protein sorting complex, ESCRT-I. *Cell* **106,** 145–155 (2001).
9. Saksena, S., Wahlman, J., Teis, D., Johnson, A. E. & Emr, S. D. Functional reconstitution of ESCRT-III assembly and disassembly. *Cell* **136,** 97–109 (2009).
10. Wollert, T., Wunder, C., Lippincott-Schwartz, J. & Hurley, J. H. Membrane scission by the ESCRT-III complex. *Nature* **458,** 172–177 (2009).
11. Wollert, T. & Hurley, J. H. Molecular mechanism of multivesicular body biogenesis by ESCRT complexes. *Nature* **464,** 864–869 (2010).
12. Martin-Serrano, J., Zang, T. & Bieniasz, P. D. HIV-1 and Ebola virus encode small peptide motifs that recruit Tsg101 to sites of particle assembly to facilitate egress. *Nat. Med.* **7,** 1313–1319 (2001).
13. Garrus, J. E. *et al*. Tsg101 and the vacuolar protein sorting pathway are essential for HIV-1 budding. *Cell* **107,** 55–65 (2001).
14. Strack, B., Calistri, A., Craig, S., Popova, E. & Gottlinger, H. G. AIP1/ALIX is a binding partner for HIV-1 p6 and EIAV p9 functioning in virus budding. *Cell* **114,** 689–699 (2003).
15. Fisher, R. D. *et al*. Structural and biochemical studies of ALIX/AIP1 and its role in retrovirus budding. *Cell* **128,** 841–852 (2007).
16. Martin-Serrano, J., Eastman, S. W., Chung, W. & Bieniasz, P. D. HECT ubiquitin ligases link viral and cellular PPXY motifs to the vacuolar protein-sorting pathway. *J. Cell Biol.* **168,** 89–101 (2005).
17. Martin-Serrano, J., Yarovoy, A., Perez-Caballero, D. & Bieniasz, P. D. Divergent retroviral late-budding domains recruit vacuolar protein sorting factors by using alternative adaptor proteins. *Proc. Natl Acad. Sci. USA* **100,** 12414–12419 (2003).
18. von Schwedler, U. K. *et al*. The protein network of HIV budding. *Cell* **114,** 701–713 (2003).
19. Jouvenet, N. *et al*. Plasma membrane is the site of productive HIV-1 particle assembly. *PLoS Biol.* **4,** e435 (2006).
20. Finzi, A., Orthwein, A., Mercier, J. & Cohen, E. A. Productive human immunodeficiency virus type 1 assembly takes place at the plasma membrane. *J. Virol.* **81,** 7476–7490 (2007).
21. Welsch, S. *et al*. HIV-1 buds predominantly at the plasma membrane of primary human macrophages. *PLoS Pathog.* **3,** e36 (2007).
22. Simon, S. M. Partial internal reflections on total internal reflection fluorescent microscopy. *Trends Cell Biol.* **19,** 661–668 (2009).
23. Jouvenet, N., Bieniasz, P. D. & Simon, S. M. Imaging the biogenesis of individual HIV-1 virions in live cells. *Nature* **454,** 236–240 (2008).
24. Jouvenet, N., Simon, S. M. & Bieniasz, P. D. Imaging the interaction of HIV-1 genomes and Gag during assembly of individual viral particles. *Proc. Natl Acad. Sci. USA* **106,** 19114–19119 (2009).
25. Ivanchenko, S. *et al*. Dynamics of HIV-1 assembly and release. *PLoS Pathog.* **5,** e1000652 (2009).
26. Lin, Y., Kimpler, L. A., Naismith, T. V., Lauer, J. M. & Hanson, P. I. Interaction of the mammalian endosomal sorting complex required for transport (ESCRT) III protein hSnf7-1 with itself, membranes, and the AAA+ ATPase SKD1. *J. Biol. Chem.* **280,** 12799–12809 (2005).
27. Howard, T. L., Stauffer, D. R., Degnin, C. R. & Hollenberg, S. M. CHMP1 functions as a member of a newly defined family of vesicle trafficking proteins. *J. Cell Sci.* **114,** 2395–2404 (2001).
28. Stuchell, M. D. *et al*. The human endosomal sorting complex required for transport (ESCRT-I) and its role in HIV-1 budding. *J. Biol. Chem.* **279,** 36059–36071 (2004).
29. Zamborlini, A. *et al*. Release of autoinhibition converts ESCRT-III components into potent inhibitors of HIV-1 budding. *Proc. Natl Acad. Sci. USA* **103,** 19140–19145 (2006).
30. Goila-Gaur, R., Demirov, D. G., Orenstein, J. M., Ono, A. & Freed, E. O. Defects in human immunodeficiency virus budding and endosomal sorting induced by TSG101 overexpression. *J. Virol.* **77,** 6507–6519 (2003).
31. Morita, E. *et al*. Human ESCRT-III and VPS4 proteins are required for centrosome and spindle maintenance. *Proc. Natl Acad. Sci. USA* **107,** 12889–12894 (2010).
32. Morita, E. *et al*. Human ESCRT and ALIX proteins interact with proteins of the midbody and function in cytokinesis. *Embo J.* **26,** 4215–4227 (2007).
33. Carlton, J. G. & Martin-Serrano, J. Parallels between cytokinesis and retroviral budding: a role for the ESCRT machinery. *Science* **316,** 1908–1912 (2007).
34. VerPlank, L. *et al*. Tsg101, a homologue of ubiquitin-conjugating (E2) enzymes, binds the L domain in HIV type 1 Pr55(Gag). *Proc. Natl Acad. Sci. USA* **98,** 7724–7729 (2001).
35. Usami, Y., Popov, S. & Gottinger, H. G. Potent rescue of human immunodeficiency virus type 1 late domain mutants by ALIX/AIP1 depends on its CHMP4 binding site. *J. Virol.* **81,** 6614–6622 (2007).
36. Carlton, J. G., Agromayor, M. & Martin-Serrano, J. Differential requirements for Alix and ESCRT-III in cytokinesis and HIV-1 release. *Proc. Natl Acad. Sci. USA* **105,** 10541–10546 (2008).
37. Zhai, Q. *et al*. Structural and functional studies of ALIX interactions with YPX(n)L late domains of HIV-1 and EIAV. *Nat. Struct. Mol. Biol.* **15,** 43–49 (2008).
38. Briggs, J. A. *et al*. The stoichiometry of Gag protein in HIV-1. *Nat. Struct. Mol. Biol.* **11,** 672–675 (2004).
39. Popov, S., Popova, E., Inoue, M. & Gottinger, H. G. Divergent Bro1 domains share the capacity to bind human immunodeficiency virus type 1 nucleocapsid and to enhance virus-like particle production. *J. Virol.* **83,** 7185–7193 (2009).
40. Dussupt, V. *et al*. The nucleocapsid region of HIV-1 Gag cooperates with the PTAP and LYPXnL late domains to recruit the cellular machinery necessary for viral budding. *PLoS Pathog.* **5,** e1000339 (2009).

METHODS

Plasmid derivation. Plasmids expressing codon-optimized HIV-1 Gag and Gag–mCherry proteins, namely pCR3.1/HIV-Gag and pCR3.1/HIV-Gag–mCherry, were previously described[23]. A derivative of pCR/HIV-1-Gag and pCR3.1/HIV-Gag–mCherry lacking the bipartite late domain in p6 (PTAP and Leu–Arg–Ser–Leu–Phe were mutated to Leu–Thr–Ala–Leu and Leu–Arg–Ser–Pro–Ser, respectively) was generated using overlapping PCR methods[41]. Plasmids expressing codon-optimized EIAV Gag/Gag–mCherry proteins (pCR3.1/EIAV-Gag and pCR3.1/EIAV-Gag-mCherry) were generated by inserting the *Gag* gene into pCR3.1 and pCR3.1/mCherry. A derivative of pCR/EIAV-Gag and pCR3.1/EIAV-Gag–mCherry in which the Alix-binding site was mutated (Tyr–Pro–Asn–Leu to Ala–Ala–Asp–Ala) was generated using overlapping PCR methods. Plasmids expressing HIV-1 viral protein U (Vpu), namely, pCR3.1/Vpu, were previously described[41].

pCR3.1-GFP–Alix, pCR3.1-GFP–Tsg101, pCR3.1-Chmp1b–GFP, pCR3.1-GFP–Chmp4b, pCR3.1-GFP–Chmp4c and pCR3.1-GFP–Vps4A were previously described[12,17] and were used to generate LNCX (Clontech; Alix, Tsg101, Chmp4b, Chmp4c and Vps4A)- or LMNI (Chmp1b)-derived retroviral vectors. LMNI is a murine leukaemia virus (MLV)-based retroviral vector in which expression of the inserted gene complementary DNA is driven by the MLV long terminal repeat and is linked to sequences encoding an internal ribosome entry site and a blasticidin-resistance gene. The plasmid encoding the Vps4 mutant E228Q, namely pCR3.1-Vps4-DN was previously described[42] and was used to generate pCR3.1-Vps4-DN–mCherry. pCR3.1-GFP–Vps4^{K173Q} was derived from pCR3.1-GFP–Vps4A by using PCR-based methods.

Cells and transfection. HeLa cells were maintained in Dulbecco's modified Eagle's medium supplemented with 10% fetal calf serum. HeLa cell lines stably expressing GFP-tagged versions of the ESCRT proteins were generated by retroviral transduction as described previously[23]. Single-cell clones expressing low levels of each GFP fusion proteins were selected for the experiments. HeLa cells were transfected with untagged Gag and Gag–mCherry in a 10:1 ratio using Lipofectamine 2000 (InVitrogen).

Multinucleation assays. Approximately 10^5 HeLa cells stably expressing GFP-tagged ESCRT proteins were plated on glass-bottomed dishes (MatTek). As a control, cells were transfected for 24 h with 1 μg of plasmid expressing either GFP alone of GFP-tagged Vps4^{K173Q}, whose overexpression is known to inhibit cytokinesis[32]. Cells were fixed and stained with anti-α-tubulin antibodies and with 4,6-diamidino-2-phenylindole (DAPI). Three-hundred cells from three independent experiments were analysed for the presence of more than one nucleus per cell. Cells connected by midbodies were considered multinucleated.

Virus release assays and western blot analysis. VLP release assays were carried as previously described[43] by transfecting approximately 3×10^6 cells in 10-cm dishes with 2 μg of Gag and 1 μg of Vpu expression plasmids. Cells and extracellular virus particles were collected at 24 h as described previously[41]. Virion and cell lysates were separated on 4–12% acrylamide gels, and proteins were probed with various antibodies: anti-Vps4A (UT2889, 1:1,000 dilution)[18], anti-Alix (1:1,000 dilution; gifts from W. Sundquist)[15], anti-HIV-1 p24CA (183-H12-5C, 1:100 dilution), anti-EIAV equine serum (1:200 dilution; VMRD) and anti-GFP (1:5,000 dilution; Roche). Blots were subsequently probed with anti-horse and anti-mouse antibodies (1:10,000 dilution) conjugated to IRDye680 (LI-COR Biotechnology). Fluorescent signals were detected using a LI-COR Odyssey scanner (LI-COR Biotechnology).

Image acquisition. For microscopic analysis, HeLa cells were plated on glass-bottomed dishes (MatTek) and transfected with a total of 1 μg of plasmids expressing Gag/Gag–mCherry, as described above. For epifluorescence microscopy, cells were fixed 18–20 h after transfection and nuclei were stained with DAPI, as previously described[41], and/or with a mouse antibody against α-tubulin (clone B-512, 1:10,000 dilution; Sigma) followed by an anti-mouse Alexa Fluor 594 (Molecular Probes). Fluorescent imaging of fixed cells was done using a Deltavision microscopy suite, as previously described[41].

Live-cell TIR-FM was carried out as previously described[23,24], with an inverted Olympus IX-70 microscope with a ×60, 1.45 NA TIR objective (Olympus Scientific) and a 12-bit cooled charge-coupled device (CCD) camera (ORCA-ER; Hamamatsu Photonics). Cells were imaged 5–8 h after transfection. The microscope was enclosed in a home-built chamber and all imaging was carried out at 37 °C. The evanescent field decayed to $1/e$ in 70 nm. Simultaneous dual-colour TIR-FM imaging of GFP and mCherry was achieved by exciting GFP with the 488-nm laser line of an argon laser (Omnichrome; Melles Griot) and red fluorescent proteins with a 543-nm HeNe laser (model 05-LGR-193, Melles Griot) reflected off a 488/543 polychroic mirror. The emission was spectrally separated by means of an emission splitter (Dual-View; Optical Insights) equipped with a 515/30 band-pass filter and a 580 long-pass filter. All mirrors and filters were obtained from Chroma Technologies. Time-lapse movies were acquired over a 30–60 min period with one image acquired every 5 s, as previously described[23,24]. The camera and shutters were controlled using MetaMorph software (Molecular Devices).

Data analysis. All data analyses used MetaMorph software. For dual-colour movie sequences, the images acquired through the emission splitter were separated, aligned with an accuracy of a single pixel, and analysed. For measuring the intensity of fluorescent puncta, a region of 8×8 pixels was drawn around an area of interest and the maximum fluorescent intensity within this region recorded. The time to complete assembly was defined as the elapsed time from the image at which a fluorescent Gag signal is first detectable to the point when Gag intensity reaches a plateau.

For analysis of co-localization, regions of 8×8 pixels were drawn around VLPs, which were selected in the Gag–mCherry channel (red), and the fluorescent intensity in the corresponding region in the GFP–ESCRT protein channel (green) was recorded. Alternatively, GFP-positive puncta were selected and the fluorescent intensity in the corresponding region in the Gag–mCherry protein channel (red) was recorded. The fluorescent intensities in both channels were quantified and transferred to Excel for analysis.

Fluorescence-activated cell sorting analysis. The distribution of GFP expression of HeLa cells and HeLa cells expressing GFP-tagged ESCRT proteins was analysed with a BD LSRII FACS. Approximately 100,000 cells were analysed per cell line.

Statistical analysis. Error bars in Fig. 2a,b indicate standard deviation calculated with Excel using: $\sqrt{\sum (x - \bar{x})^2 / (n-1)}$

41. Neil, S. J., Eastman, S. W., Jouvenet, N. & Bieniasz, P. D. HIV-1 Vpu promotes release and prevents endocytosis of nascent retrovirus particles from the plasma membrane. *PLoS Pathog.* **2**, e39 (2006).
42. Martin-Serrano, J., Zang, T. & Bieniasz, P. D. Role of ESCRT-I in retroviral budding. *J. Virol.* **77**, 4794–4804 (2003).
43. Jouvenet, N. *et al.* Broad-spectrum inhibition of retroviral and filoviral particle release by tetherin. *J. Virol.* **83**, 1837–1844 (2009).
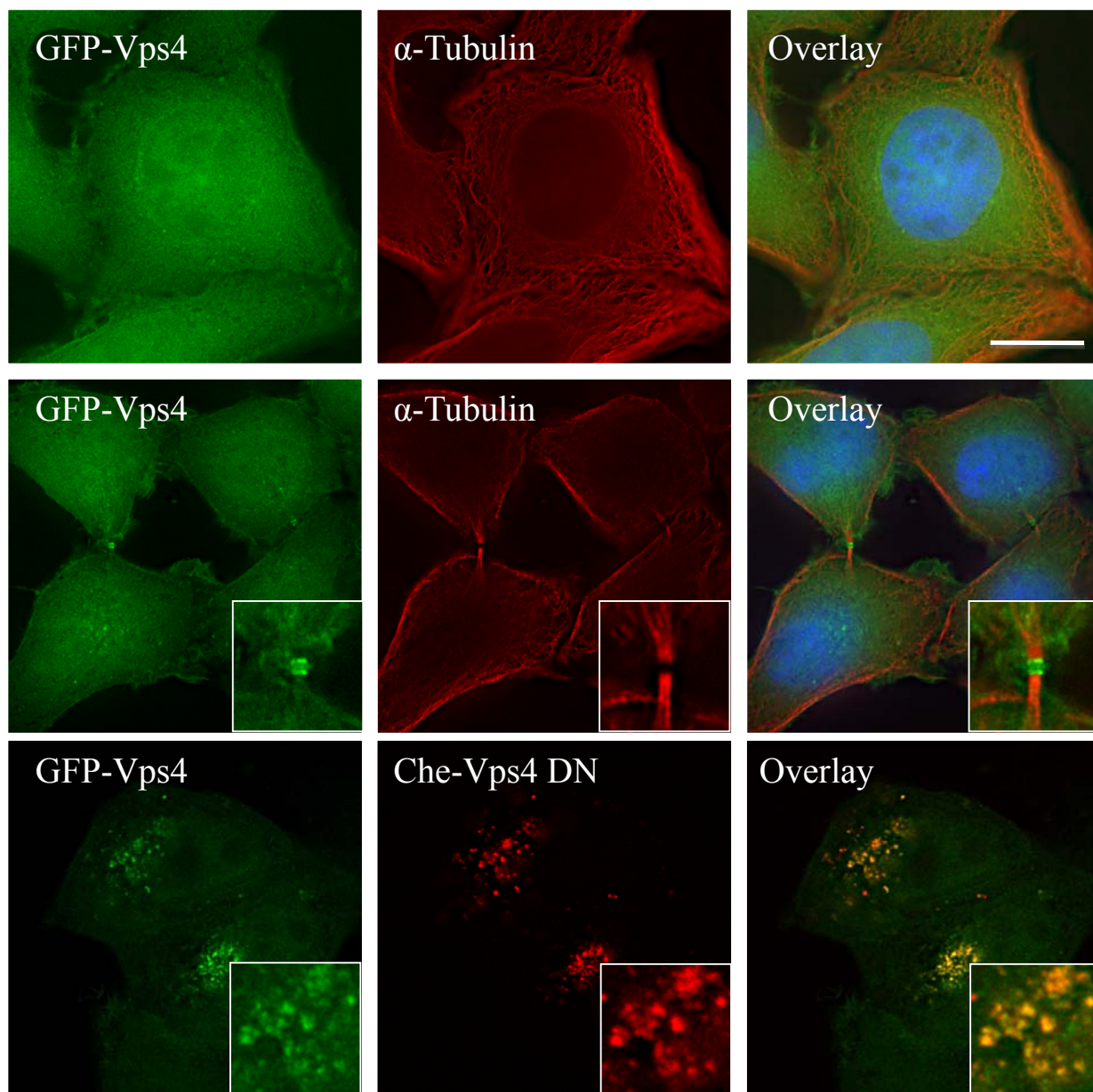
DOI: 10.1038/ncb2207
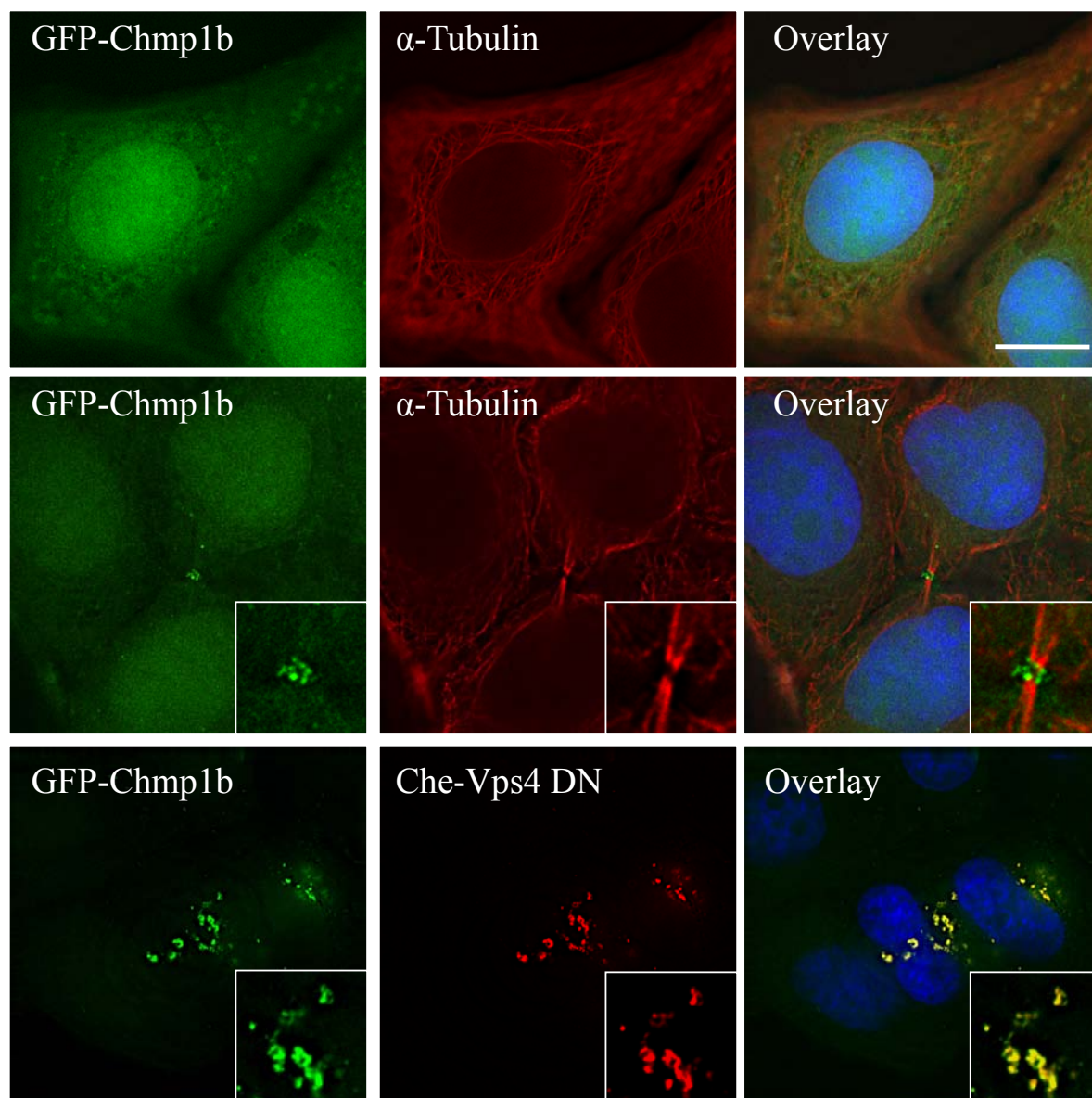
Figure S1 Characterization of the Chmp1b-GFP-expressing cell clone. Hela cells stably expressing Chmp1b-GFP (green) were fixed and stained with anti-a-tubulin antibodies (red) and with DAPI (blue). Images show the distribution of Chmp1-GFP in interphase cells (top panels) and in telophase cells (middle panels). Alternatively, cells were transfected with Vps4-DN-mCherry (bottom panels), fixed 18 hours post-transfection and stained with DAPI (blue).Samples were observed with an epifluorescence microscope. Deconvolved optical sections acquired at the center of the vertical dimension of the cell are shown. Expanded views are shown in insets. The scale bars represent 10μm.
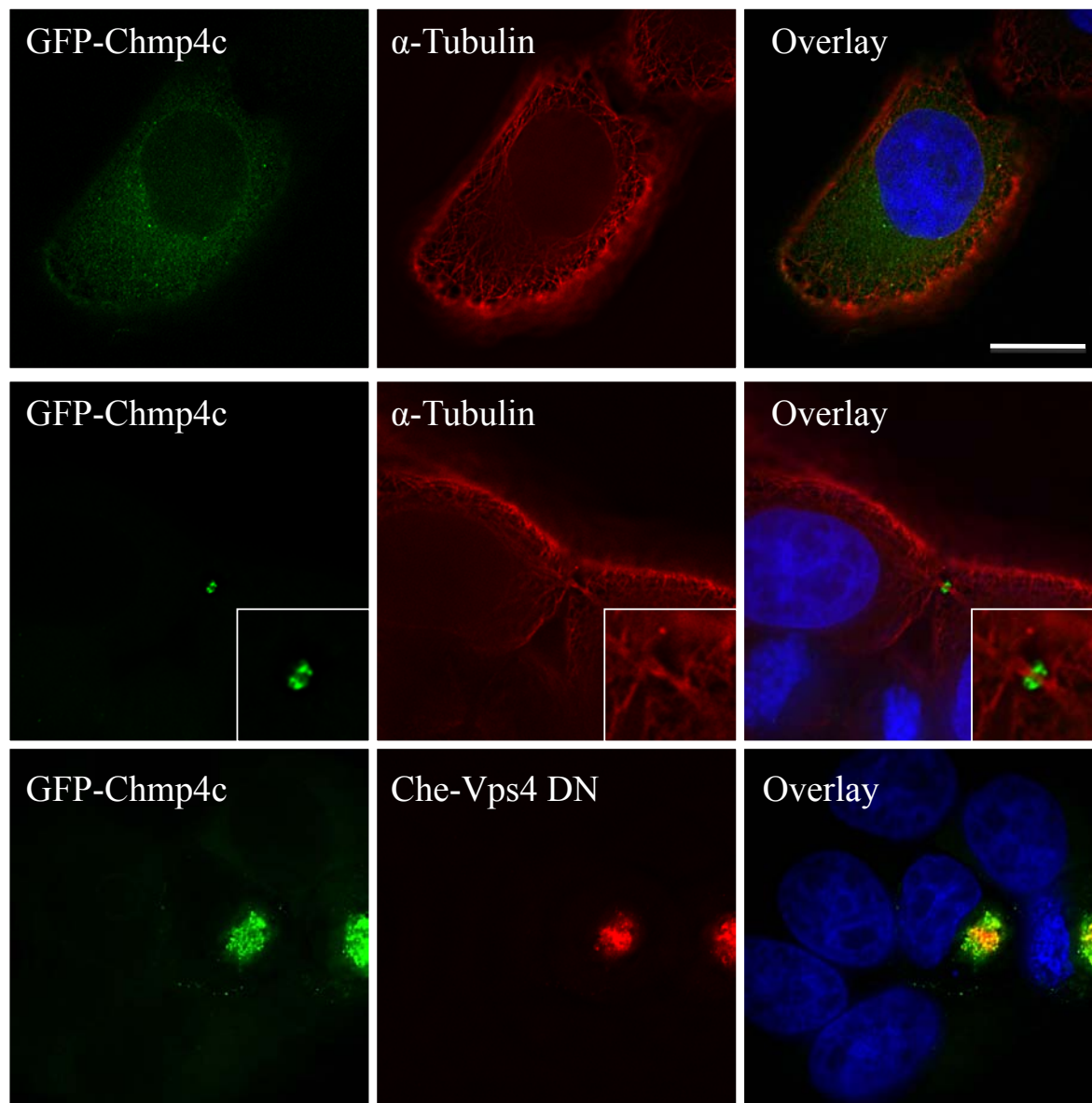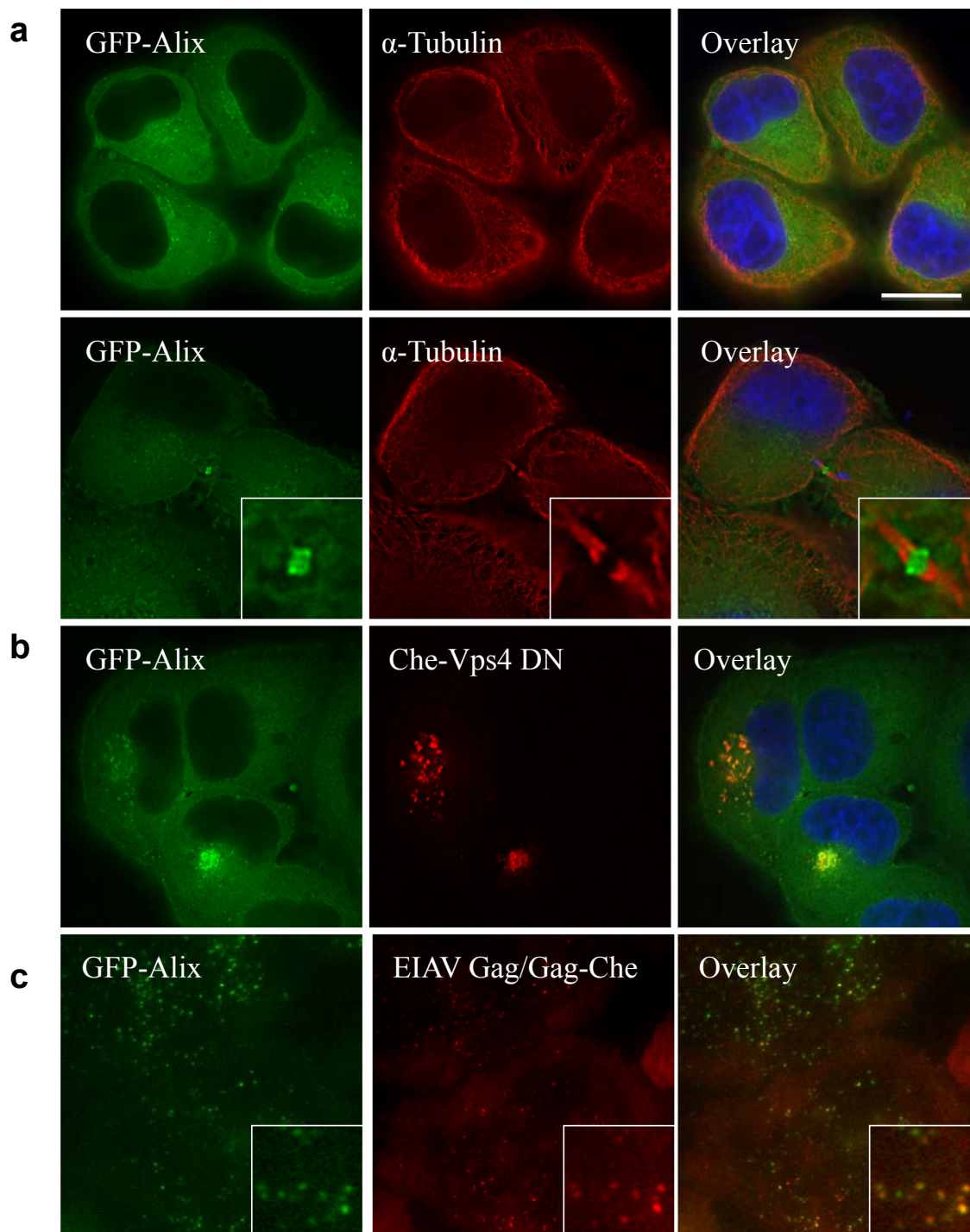
Figure S2 Characterization of the GFP-Chmp4c-expressing cell clone. Hela cells stably expressing GFP-Chmp4c (green) were fixed and stained with anti-a-tubulin antibodies (red) and with DAPI (blue). Images show the distribution of GFP-Chmp4c in interphase cells (top panels) and in telophase cells (middle panels). Alternatively, cells were transfected with Vps4-DN-mCherry (bottom panels), fixed 18 hours post-transfection and stained with DAPI (blue). Samples were observed with an epifluorescence microscope. Deconvolved optical sections acquired at the center of the vertical dimension of the cell are shown. Expanded views are shown in insets. The scale bars represent 10μm.

Figure S3 Characterization of the GFP-Vps4A-expressing cell clone. Hela cells stably expressing GFP-Vps4A (green) were fixed and stained with anti-a-tubulin antibodies (red) and with DAPI (blue). Images show the distribution of GFP-Vps4A in interphase cells (top panels) and in telophase cells (middle panels). Alternatively, cells were transfected with Vps4-DN-mCherry (bottom panels), fixed 18 hours post-transfection and stained with DAPI (blue). Samples were observed with an epifluorescence microscope. Deconvolved optical sections acquired at the center of the vertical dimension of the cell are shown. Expanded views are shown in insets. The scale bars represent 10μm.

Figure S4 Characterization of the GFP-Alix-expressing cell clone. a. Hela cells stably expressing GFP-Alix (green) were fixed and stained with anti-a-tubulin antibodies (red) and with DAPI (blue). Images show the distribution of GFP-Alix in interphase cells (top panels) and in telophase cells (bottom panels). b. Cells were transfected with Vps4A-DN-mCherry, fixed 18 hours post-transfection and stained with DAPI. c. Cells were transfected with EIAV Gag/Gag-mCherry fixed 18 hours post-transfection and stained with DAPI (blue). In panels (a) and (b) images are deconvolved optical sections acquired at the center of the vertical dimension of the cell with an epifluorescent microscope. (c) panels are TIR-FM images. Expanded views are shown in insets. The scale bars represent 10µm.
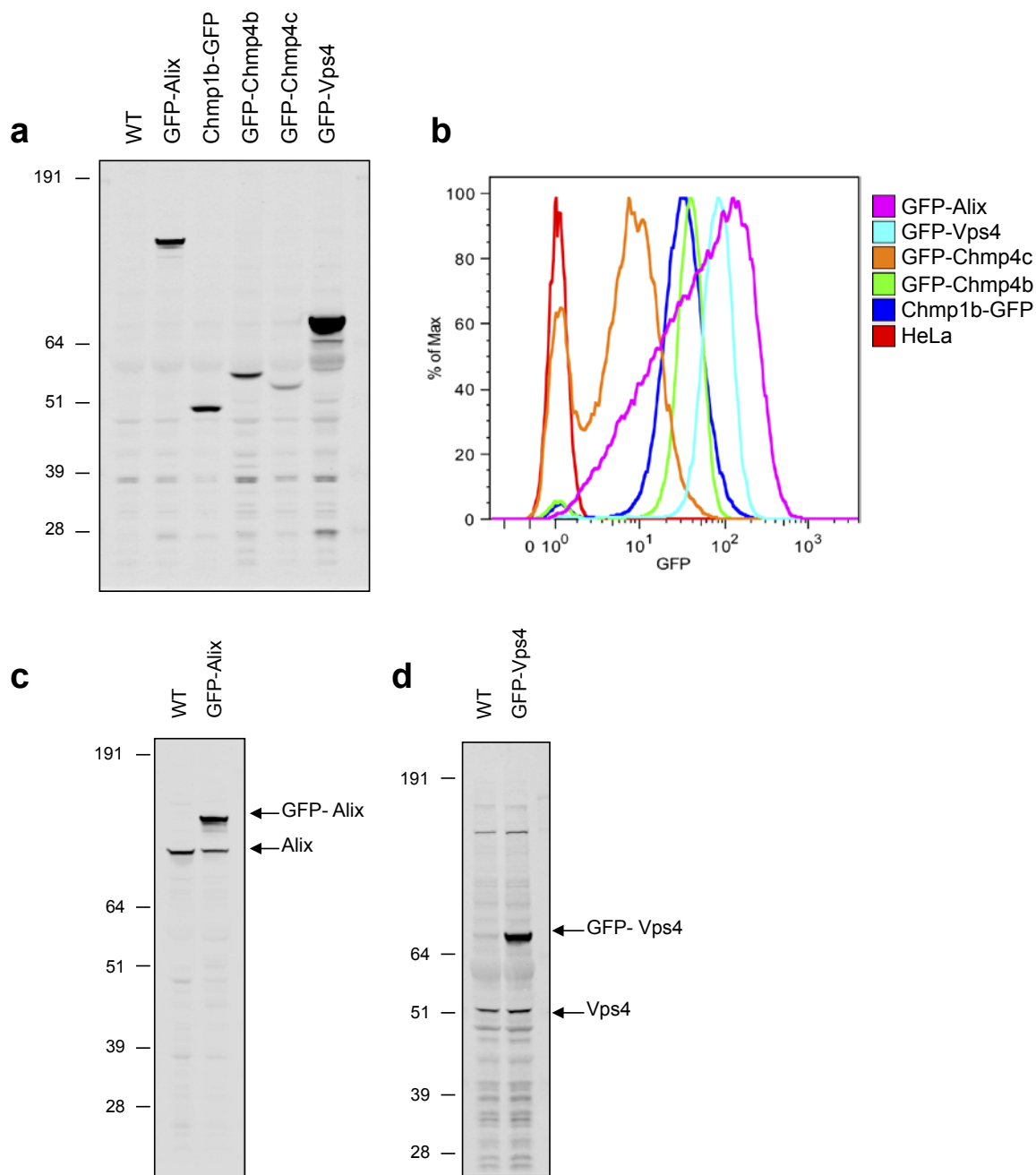
Figure S5 Characterization of the level of expression of GFP-tagged ESCRT in the stable cell clones. a. Western blot analysis of unmodified Hela cells and Hela cells stably expressing the indicated GFP-tagged ESCRT proteins probed with an anti-GFP monoclonal antibody. b. FACS analysis of GFP fluorescence in unmodified Hela cells and Hela cells stably expressing the indicated GFP-tagged ESCRT proteins. c.Western blot analysis of unmodified Hela cells and Hela cells stably expressing GFP-Alix probed with an anti-Alix antiserum. d. Western blot analysis of unmodified Hela cells and Hela cells stably expressing GFP-Vps4 probed with anti-Vps4 antiserum. The scale to the left of each blot represents the positions of molecular weight markers (in kDa)
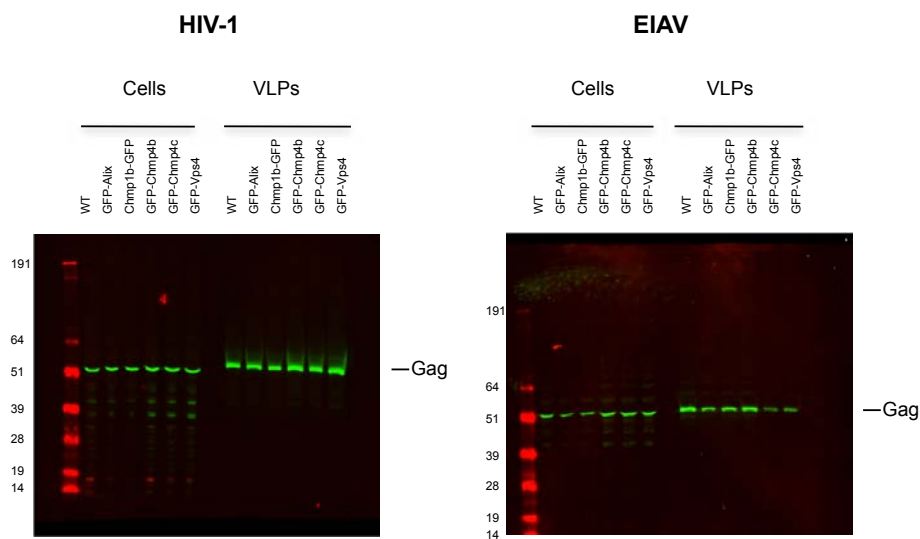
Figure S6 Full scans of western blots shown in figure 2d. Molecular weight markers are indicated in kDa.